

# The Relationship Between Extraordinary Optical Transmission and Surface-Enhanced Raman Scattering in Subwavelength Metallic Nanohole Arrays

Qianhong Li<sup>1</sup>, Zhilin Yang<sup>1,2,\*</sup>, Bin Ren<sup>3</sup>, Hongxing Xu<sup>2</sup>, and Zhongqun Tian<sup>3</sup>

<sup>1</sup>Department of Physics, Xiamen University, Xiamen, 361005, China

<sup>2</sup>Institute of Physics, Chinese Academy of Sciences, Beijing, 100190, China

<sup>3</sup>State Key Laboratory of Physical Chemistry of Solid Surfaces and Department of Chemistry, College of Chemistry and Chemical Engineering, Xiamen University, Xiamen, 361005, China

Nanohole arrays in an Ag film were used as a substrate for surface-enhanced Raman scattering in the optical range. Extraordinary optical transmission and local field enhancement in Ag nanohole arrays were theoretically simulated using three-dimensional finite difference time domain method. The periodicity of the holes was adjusted to control the transmission intensity and electric field intensity. The calculation results show that the peak position of transmission red-shifts as the periodicity increases, while the peak intensity decreases linearly. The electric field is localized in a very small region at the edges of the holes, which means the surface-enhanced Raman scattering originates only from a small number of molecules located in the edge regions. The electric field intensity changes with the excitation wavelength in a similar trend to the transmission intensity. Both the electric field intensity and transmission intensity reach their maximum value at the frequency of surface plasmon resonance. The structure that gives resonant transmission provides the maximum surface-enhanced Raman scattering signal. Controllable and predictable surface-enhanced Raman scattering can be produced by using this novel nanostructure. The structure can be optimized to get the maximum surface-enhanced Raman scattering signal at a certain excitation wavelength through numerical simulations.

**Keywords:** Nanohole Arrays, Extraordinary Optical Transmission, Surface-Enhanced Raman Scattering, Surface Plasmons.

## 1. INTRODUCTION

Extraordinary optical transmission (EOT) through nanohole arrays in the metal film was first reported in 1998 by Ebbesen et al.<sup>1</sup> Since this pioneering experimental work, the EOT has attracted great interest in its underlying physical mechanism<sup>2–13</sup> and its potential application.<sup>14–26</sup> It has been shown that geometric factors, such as the periodicity of the hole arrays, the film thickness and the shape and size of the holes,<sup>1,5,7–9</sup> play critical roles in this effect. It is widely recognized the EOT effect is mainly due to the coupling of light with surface plasmons (SP) on the periodically patterned metal film.<sup>1,2,4,8,9,11</sup> The conversion from photon to SP and back to photon through nanohole arrays is a simplified interpretation of the EOT mechanism.

Because of the field localization properties of EOT, this nanostructure can be used as a promising substrate for surface-enhanced Raman scattering (SERS) in the optical range.<sup>18,23</sup> The main challenge in SERS is to get reproducible spectra which is fairly important for a reliable quantitative analysis. Conventional SERS from metallic particles have the disadvantage of unpredictable local field enhancements, which has limited the application of SERS to wider scientific fields. To overcome this limitation, a lot of efforts have been devoted to obtain SERS from periodic nanostructure recently.<sup>18–26</sup> A primary motivation of exploring SERS in nanohole arrays is to obtain uniform and stable “hot spot”, located in a small region at the edges of the holes. The geometric factors can be changed to produce controllable and predictable SERS. Because of these advantages, nanohole arrays may have a promising application for ultrasensitive chemical sensing.<sup>26</sup>

\*Author to whom correspondence should be addressed.

In this work, we explored the relationship between transmission intensity and electric field intensity from nanohole arrays in an Ag film. Three-dimensional finite difference time domain (3D-FDTD) method was employed to simulate the transmission intensity and electric field intensity from the structure. A correlation between the excitation-wavelength dependent transmission intensity and SERS intensity was analyzed.

## 2. CALCULATION METHOD

FDTD is a kind of numerical method for simulating electromagnetic field first reported by Yee in 1966.<sup>27</sup> The electromagnetic field and structural material are described on a discrete mesh made up of so-called Yee cells. The core of FDTD method is to solve Maxwell's equations discretely in time and space.

3D-FDTD shows great advantages in simulating of complex system interacting with light. Lumerical FDTD solutions software (FDTD Solutions 6.0) was used to calculate the transmission intensity and electric field intensity in this work. Figure 1 presents a view of nanohole arrays with diameter  $d$ , thickness  $t$  and periodicity  $p$ . Boundary conditions in this simulation are periodic boundary conditions along the  $x$  and  $y$  directions and perfectly matched layer along the  $z$  direction. Simulation time was set to be 1000 fs which is usually long enough for simulation, and the simulation will shutoff automatically when the fields have decayed. Mesh accuracy was set at 5 for overall simulation region and smaller mesh was chosen around the holes. The appropriate grid size was chosen to help simulate more accurately and save simulation time. Nanohole arrays were excited by plane wave along the  $z$  direction and polarization was set parallel to  $x$  axis. Frequency domain power monitor and frequency domain profile monitor for the transmission and electromagnetic field respectively were placed on the transmitted surface. The frequency

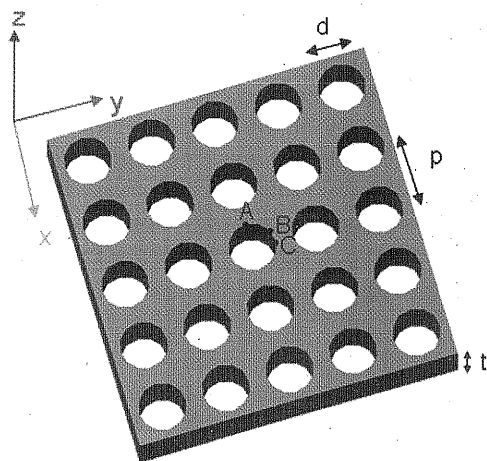


Fig. 1. Schematics of nanohole arrays in an Ag film with diameter  $d$ , thickness  $t$  and periodicity  $p$ .

dependent complex relative permittivity of silver is characterized by Drude model  $\epsilon_m(\omega) = \epsilon - \omega_p^2 / (\omega(i\gamma + \omega))$ .<sup>28</sup>

## 3. RESULTS AND DISCUSSION

Figure 2(a) shows the transmission spectra of nanohole arrays with different holes periodicities (from 420 nm to 620 nm) at  $d = 225$  nm,  $t = 220$  nm. It is observed that the peak position of transmission red-shifts and the peak intensity decreases with the increase of the periodicity of the

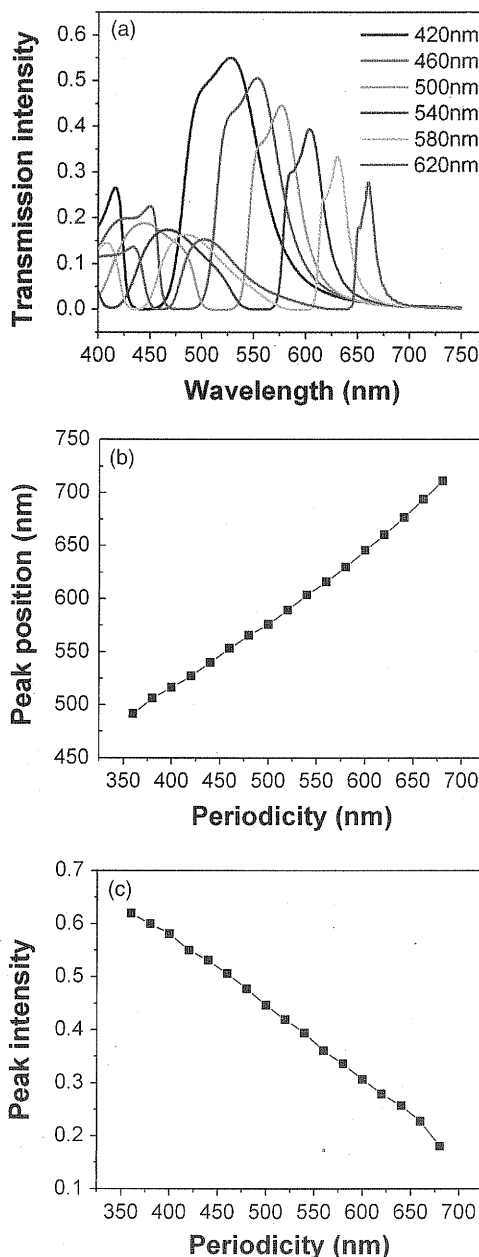


Fig. 2. (a) Calculated transmission spectra through the nanohole arrays with different periodicities (from 420 nm to 620 nm). (b) and (c) show dependences of peak position and peak intensity on the periodicity ( $d = 225$  nm,  $t = 220$  nm).

holes. The shape of the peak is also changed with periodicity, with sharper and narrower peaks at longer periodicities. This phenomenon can be understood by the contributions from the modes of the surface plasmon polariton (SPP) and the localized surface plasmon (LSP).<sup>9</sup> The LSP peak is only visible when it significantly overlaps with an SPP peak, and when the SPP peak is on the left-hand side, the transmission associated with the LSP is blocked due to the destructive interference. The cut-off function of the subwavelength aperture arrays leads to a drop in the peak intensity at longer wavelength.<sup>9</sup> When the incident wavelength is longer than the cut-off wavelength, the transmission decreases significantly as expected for such a tunneling phenomena.<sup>12</sup>

Figures 2(b, c) intuitively show dependences of peak position and peak intensity of transmission on the periodicity respectively. The peak position red-shifts and peak intensity decreases linearly with the increase of the periodicity. The slope of curve in Figure 2(b) is about  $\Delta\lambda_{\text{peak}}/\Delta P = 0.64$ .

At normally incident, the wavelength of SPP resonance ( $\lambda_{\text{sp}}$ ) from nanohole arrays can be estimated by the following equation:<sup>2</sup>

$$\lambda_{\text{sp}}(i, j) = \frac{P}{\sqrt{i^2 + j^2}} \sqrt{\frac{\epsilon_d \epsilon_m}{\epsilon_d + \epsilon_m}} \quad (1)$$

Where  $P$  is the lattice constant (periodicity) of the arrays,  $i$  and  $j$  are integers that are related to the scattering orders of the arrays,  $\epsilon_d$  and  $\epsilon_m$  are the real part of dielectric constants of the adjacent medium and the metal, respectively. The transmission spectra of arrays with different periodicities in Figure 2(a) shows peak positions slightly red-shift compared to this equation. This is because the equation only takes a resonant contribution (SP excitation) into account and neglects the non-resonant contribution (direct scattering).<sup>6</sup>

Figure 3 shows the electrical field ( $|E|^2$ ) distribution at the transmitted surface of the nanohole arrays at 632 nm excitation. It is clear that the highest electric field is localized in a very small region at the aperture edges on the air/silver side, and the SERS signal originates mainly from molecules located in the edge regions. In this aspect, nanohole arrays in the Ag film appears to be a useful platform for enhanced spectroscopy at least for the following two reasons: they provide the strong electromagnetic field necessary for the surface enhanced spectroscopy and restrict the molecules to be detected to a very small volume at the edges of the holes.

Figure 4 shows the relationship between transmission intensity and electric field intensity. Three points (A, B, C) marked in Figure 1 at the transmitted surface were chosen to calculate their electric field intensity over the whole spectral range interested. From the figure, we can see that the electric field intensity at point A is the strongest compared with points B and C, which can be easily understood

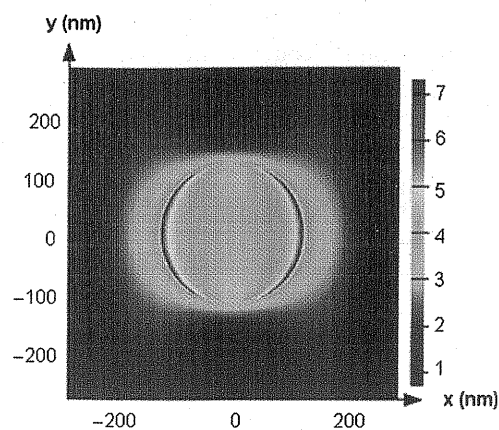


Fig. 3. Calculated electric field intensity ( $|E|^2$ ) at the transmitted surface of nanohole arrays with  $p = 582$  nm,  $d = 250$  nm and  $t = 340$  nm at 632 nm excitation and the value of field intensity took the natural logarithm. Polarization of incident beam is parallel to the  $x$  axis.

by considering the  $x$ -polarization of the incident beam. Although the electric field intensity of three points is different, the peak position is the same. They all achieve maximum field intensity at 632 nm. To compare more clearly, transmission intensity was multiplied by a factor of 200. It is observed that the peak position of transmission is also at 632 nm, and the electric field intensity can get maximum value with 632 nm excitation using this structure. Because the SERS enhancement is considered to be proportional to the fourth power of the field enhancement ( $|E|^4$ ),<sup>29,30</sup> it is obviously that the structure that gives resonant transmission at the excitation wavelength provides the maximum SERS signal.

SP excitations lead to a concentration of the electrons at the surface on the sub-wavelength scale. When the SP resonance condition is achieved, the EOT phenomenon appears. That is to say SP plays an essential role in the EOT from the nanohole arrays. Since the electric field enhancement accounts for the majority of SERS signal, SP is responsible for both EOT and SERS from the nanohole

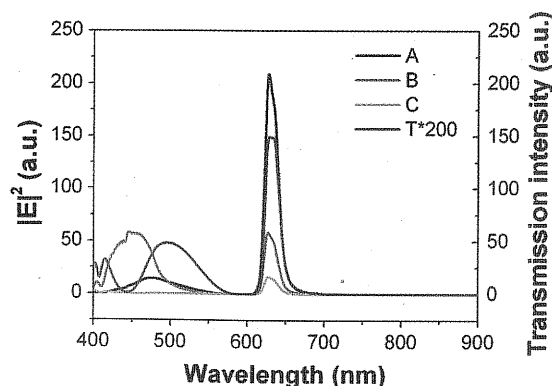


Fig. 4. Calculated electric field intensity of three points (A, B, C) refers to that in Fig. 1) and transmission intensity ( $T$ , multiplied by 200) at the transmitted surface over the spectral range of 400 nm to 900 nm from nanohole arrays with  $p = 582$  nm,  $d = 250$  nm and  $t = 340$  nm.

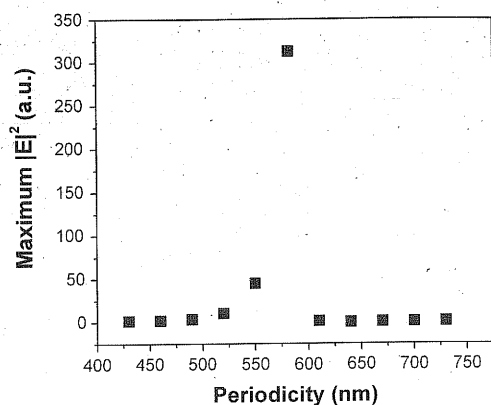


Fig. 5. Maximum value of electric field intensity ( $|E|^2$ ) for each array plotted as a function of holes periodicity with a fixed hole diameter and film thickness ( $d = 250$  nm,  $t = 340$  nm).

arrays. A same mechanism results in two different effects, so the two effects have close relationship. When the SP resonance condition is achieved, transmission intensity and SERS signal can reach the greatest value at the same excitation wavelength.

Figure 5 shows the dependence of the maximum electric field intensity ( $|E|^2$ ) on the hole periodicity when the hole diameter and the film thickness are fixed ( $d = 250$  nm and  $t = 340$  nm). The electric field intensity from the arrays with 582 nm periodicity is maximized at the 632 nm excitation, whereas the electric field intensity from the arrays with other periodicity is much lower. This result is similar to the calculated result from nanohole arrays in a copper film<sup>23</sup> and can be easily understood from Eq. (1). Because the highest electric field will be achieved from the arrays with resonant transmission at the laser excitation, it is reasonable that the maximum electric field intensity will be achieved from a specific periodicity arrays at a specific excitation wavelength.

#### 4. CONCLUSIONS

Extraordinary optical transmission and local field enhancement was simulated using 3D-FDTD method. The periodicity of the arrays was varied to discuss its influence on EOT and SERS. With the increase of the periodicity, the peak position of transmission increases and the peak intensity decreases linearly. The enhanced field is localized in a very small region at the aperture edges on the air/silver side, providing strong SERS enhancement. Transmission intensity and electric field intensity get their maximum value at the same excitation frequency when the conditions of SP resonance are satisfied. The result gives a direct correlation between EOT and SERS and indicates that SERS substrates with reliable and predictable strong enhancement can be obtained by optimizing the periodicity of the nanohole arrays.

**Acknowledgments:** This work was supported by the National Natural Science Foundation of China (Grant No. 20703032), National Basic Research Project of China (Grant No.2009CB930703), Natural Science Foundation of Fujian Province of China (No.E0710028).

#### References and Notes

1. T. W. Ebbesen, H. J. Lezec, H. F. Ghaemi, T. Thio, and P. A. Wolff, *Nature* 391, 667 (1998).
2. H. F. Ghaemi, T. Thio, D. E. Grupp, T. W. Ebbesen, and H. J. Lezec, *Phys. Rev. B* 58, 6779 (1998).
3. D. E. Grupp, H. J. Lezec, T. W. Ebbesen, K. M. Pellerin, and T. Thio, *Appl. Phys. Lett.* 77, 1569 (2000).
4. L. Martín-Moreno, F. J. García-Vidal, H. J. Lezec, K. M. Pellerin, T. Thio, J. B. Pendry, and T. W. Ebbesen, *Phys. Rev. Lett.* 86, 1114 (2001).
5. A. Degiron, H. J. Lezec, W. L. Barnes, and T. W. Ebbesen, *Appl. Phys. Lett.* 81, 4327 (2002).
6. C. Genet, M. P. van Exter, and J. P. Woerdman, *Opt. Commun.* 225, 331 (2003).
7. H. Cao and A. Nahata, *Opt. Express* 12, 3664 (2004).
8. K. L. van der Molen, K. J. K. Koerkamp, S. Enoch, F. B. Segerink, N. F. van Hulst, and L. Kuipers, *Phys. Rev. B* 72, 045421 (2005).
9. A. Degiron and T. W. Ebbesen, *Pure Appl. Opt.* 7, S90 (2005).
10. G. Gay, O. Alloschery, B. V. de Lesegno, C. O'Dwyer, J. Weiner, and H. J. Lezec, *Nature Phys.* 2, 262 (2006).
11. H. W. Gao, J. Henzie, and T. W. Odom, *Nano Lett.* 6, 2104 (2006).
12. C. Genet and T. W. Ebbesen, *Nature* 445, 39 (2007).
13. H. T. Liu and P. Lalanne, *Nature* 452, 728 (2008).
14. A. G. Brolo, R. Gordon, B. Leathem, and K. L. Kavanagh, *Langmuir* 20, 4813 (2004).
15. X. G. Luo and T. Ishihara, *Appl. Phys. Lett.* 84, 4780 (2004).
16. M. P. Murray-Methot, N. Menegazzo, and J. F. Masson, *Analyst* 133, 1714 (2008).
17. J. C. Sharpe, J. S. Mitchell, L. Lin, N. Sedoglavich, and R. J. Blaikie, *Anal. Chem.* 80, 2244 (2008).
18. A. G. Brolo, E. Arctander, R. Gordon, B. Leathem, and K. L. Kavanagh, *Nano Lett.* 4, 2015 (2004).
19. J. T. Bahns, F. N. Yan, D. L. Qiu, R. Wang, and L. H. Chen, *Appl. Spectrosc.* 60, 989 (2006).
20. A. Lesuffleur, L. K. S. Kumar, A. G. Brolo, K. L. Kavanagh, and R. Gordon, *J. Phys. Chem. C* 111, 2347 (2007).
21. T. H. Reilly, S. H. Chang, J. D. Corbman, G. C. Schatz, and K. L. Rowlen, *J. Phys. Chem. C* 111, 1689 (2007).
22. Q. M. Yu and G. Golden, *Langmuir* 23, 8659 (2007).
23. J. R. Anema, A. G. Brolo, P. Marthandam, and R. Gordon, *J. Phys. Chem. C* 112, 17051 (2008).
24. Q. M. Yu, P. Guan, D. Qin, G. Golden, and P. M. Wallace, *Nano Lett.* 8, 1923 (2008).
25. Q. Min, M. J. L. Santos, E. M. Girotto, A. G. Brolo, and R. Gordon, *J. Phys. Chem. C* 112, 15098 (2008).
26. R. Gordon, D. Sinton, K. L. Kavanagh, and A. G. Brolo, *Acc. Chem. Res.* 41, 1049 (2008).
27. K. S. Yee, *IEEE Trans. Antennas Propag.* 14, 302 (1966).
28. U. Kreibig and M. Vollmer, *Optical Properties of Metal Clusters*, Springer, Berlin (1995).
29. M. Moskovits, *J. Raman Spectrosc.* 36, 485 (2005).
30. E. C. Le Ru, P. G. Etchegion, and M. Meyer, *J. Chem. Phys.* 125, 204701 (2006).

Received: 4 September 2009. Accepted: 30 October 2009.

RESEARCH ARTICLE